Two-Color STED Microscopy of Living Synapses Using A Single Laser-Beam Pair

Jan Tønnesen,[†‡△] Fabien Nadrigny,[†‡△] Katrin I. Willig,[§] Roland Wedlich-Söldner,[¶] and U. Valentin Nägerl[†‡*]
[†]Interdisciplinary Institute for Neuroscience, Université de Bordeaux, Bordeaux, France; [‡]UMR 5297, Centre National de la Recherche Scientifique, Bordeaux, France; [§]Max Planck Institute for Biophysical Chemistry, Göttingen, Germany; and [¶]Max Planck Institute of Biochemistry, Martinsried, Germany

ABSTRACT The advent of superresolution microscopy has opened up new research opportunities into dynamic processes at the nanoscale inside living biological specimens. This is particularly true for synapses, which are very small, highly dynamic, and embedded in brain tissue. Stimulated emission depletion (STED) microscopy, a recently developed laser-scanning technique, has been shown to be well suited for imaging living synapses in brain slices using yellow fluorescent protein as a single label. However, it would be highly desirable to be able to image presynaptic boutons and postsynaptic spines, which together form synapses, using two different fluorophores. As STED microscopy uses separate laser beams for fluorescence excitation and quenching, incorporation of multicolor imaging for STED is more difficult than for conventional light microscopy. Although two-color schemes exist for STED microscopy, these approaches have several drawbacks due to their complexity, cost, and incompatibility with common labeling strategies and fluorophores. Therefore, we set out to develop a straightforward method for two-color STED microscopy that permits the use of popular green-yellow fluorescent labels such as green fluorescent protein, yellow fluorescent protein, Alexa Fluor 488, and calcein green. Our new (to our knowledge) method is based on a single-excitation/STED laser-beam pair to simultaneously excite and quench pairs of these fluorophores, whose signals can be separated by spectral detection and linear unmixing. We illustrate the potential of this approach by two-color superresolution time-lapse imaging of axonal boutons and dendritic spines in living organotypic brain slices.

INTRODUCTION

Stimulated emission depletion (STED) microscopy is a recently developed optical technique that breaks the classic resolution limit of light microscopy (1,2). It offers the ability to shed light on cell biological processes inside neurons and synapses that have been out of reach for confocal and two-photon microscopy, whose spatial resolution is limited by the diffraction of light.

From initial applications looking at immunohistochemically labeled proteins in fixed tissue preparations (3,4), the scope of the technique has been extended to live-cell imaging, e.g., resolving fast movements of single vesicles inside nerve terminals (5) and imaging the dynamic morphology of dendritic spines labeled with yellow fluorescent protein (YFP) (6). In addition, it has recently become possible to image actin dynamics in synapses with subdiffraction spatial resolution deep inside living brain slices (100 μm) with STED microscopy, opening up the use of more intact and realistic tissue preparations for nanoscale imaging (7).

Despite these advances, a considerable drawback of STED microscopy has been the difficulty in adapting it for multicolor imaging. STED microscopy requires two well-aligned laser beams, one for fluorescence excitation and another for fluorescence quenching via stimulated emission, which poses a special challenge for imaging more than one fluorophore. Nevertheless, two-color STED microscopy has been achieved by approaches that rely on using separate lasers for each fluorophore (8,9), measuring fluorescence lifetimes (10), or using photoswitchable fluorescent proteins (11). While these approaches provide superresolution images in two colors, they are technically challenging, costly and restrictive in the type of fluorophores that can be used.

However, there is a general need for multicolor solutions that integrate live-cell superresolution laser scanning microscopy with existing fluorescent labeling strategies and markers. For instance, synapse biology would benefit greatly from multicolor STED imaging, as synapses are composed of pre- and postsynaptic compartments ensheathed by glial processes, which are typically too small to be properly resolved by conventional microscopic techniques.

We set out to develop a straightforward approach to achieve two-color STED imaging in living tissues, which works for fluorescent proteins as well as synthetic dyes in popular use. The idea was to develop an approach based on spectral detection and linear unmixing of spectrally similar fluorophores. It is well known from confocal microscopy that YFP, GFP, and other synthetic fluorophores can be excited by using the same laser, and that the respective

Submitted August 16, 2011, and accepted for publication October 12, 2011.

△Jan Tønnesen and Fabien Nadrigny contributed equally to this work.

*Correspondence: valentin.nagerl@u-bordeaux2.fr

Editor: Paul Wiseman.

0006-3495/11/11/2545/8 $2.00

doi: 10.1016/j.bpj.2011.10.011

fluorescence signals can be well separated spectrally on the side of the emission using dichroic mirrors and two or more detectors together with linear unmixing algorithms (12,13). A STED approach based on this strategy for green/yellow fluorophores would offer several important advantages by 1), avoiding setup complexity by reducing the number of lasers needed; 2), providing two-color images that are intrinsically aligned without shifts due to chromatic aberrations; 3), making it possible to use common fluorescent markers for which powerful labeling strategies exist; and 4), leaving a wider spectral range available for other optical techniques such as two-photon uncaging and optogenetics.

We have developed a powerful technique for two-color superresolution imaging of synapses in living-brain slices using YFP, GFP, and two other popular synthetic dyes (Alexa Fluor 488 and calcein green). It is based on STED microscopy using only a single pair of lasers, one to excite and the other to deplete two fluorophores simultaneously. Then, their signals are separated spectrally. We show that these fluorophores can be efficiently quenched using a single STED laser with a wavelength of 595 nm and that this approach provides a lateral spatial resolution of at least 80 nm with each fluorophore. Using organotypic brain slices, we demonstrate the potential of this two-color technique by time-lapse imaging presynaptic boutons and postsynaptic spines, which are elementary functional compartments for rapid and flexible information processing in the central nervous system.

MATERIALS AND METHODS

Microscope setup

For live-cell imaging of hippocampal brain slice cultures we custom-built a STED microscope based on pulsed excitation and pulsed depletion in the visible range of the spectrum as described previously (14) (Fig. 1 *A*). A standard commercial inverted microscope (DMI 6000 CS Trino, Leica, Mannheim, Germany) equipped with a high-numerical-aperture objective lens (PL APO, 100×, oil, NA 1.4, Leica) served as a base. We used a pulsed-laser diode (PDL 800-D, Picoquant, Berlin, Germany) to deliver excitation pulses at 485-nm wavelength and of 90 ps duration. The 595-nm-wavelength laser pulses for the STED beam were produced by an optical parametric oscillator (OPO BASIC Ring fs RTP, APE, Berlin, Germany) pumped by a Ti:Sapphire laser (MaiTai, Spectra-Physics, Darmstadt, Germany), operating at 80 MHz and emitting at $\lambda = 801$ nm. The pulses of originally 200 fs duration were stretched to ~300 ps by dispersion in a glass rod 25 cm long (SF6) and then in a polarization-preserving fiber (Schäfter & Kirchhoff, Hamburg, Germany) of 100 m length. The maximal power of the STED beam going into the back aperture of the objective was 42 mW. To create the STED focal doughnut, a polymeric phase plate (RPC Photonics, Rochester, NY) was introduced into the path of the expanded STED beam, imprinting a helical-phase ramp of $\exp(i\phi)$, with $0 < \phi < 2\pi$, onto the wavefront. The STED and excitation pulses were synchronized at 80 MHz via external triggering of the laser diode using an electronic delay generator. The laser beams were combined using a dichroic mirror (AHF Analysentechnik, Tübingen, Germany). We used a telecentric beam scanner (Yanus IV, TILL Photonics, Gräfelfing, Germany) in combination with scan and tube lenses from the microscope manufacturer to scan the laser beams across the sample. Episcopic fluorescence was first separated from the excitation by a dichroic mirror (499-nm long-pass), then cleaned with a 525/50 band-pass filter, spectrally separated by a dichroic mirror (514-nm long-pass), and finally imaged onto two multimode optical fibers connected to avalanche photodiodes (SPCM-AQR-13-FC, PerkinElmer, Waltham, MA). Image acquisition was controlled by the custom-written software IMSpector (15). As the wavelengths of the excitation (485 nm) and STED (~595 nm) lasers are >100 nm apart, there is a wide spectral band that can be used for fluorescence detection of one or more fluorophores (Fig. 1 *B*).

Animals

Wild-type and transgenic mice expressing either YFP or enhanced GFP under the Thy1 promoter (Thy1-YFP, Thy1-GFP) were kept under 12 h light/12 h dark cycle with ad libitum access to food and water (both strains from Jackson Labs, Bar Harbor, ME). All experiments were in accordance with the National Code of Ethics on Animal Experimentation (Carte Nationale d'éthique sur l'expérimentation animale; Ministère de l'enseignement et de la recherche, Ministère de l'agriculture et de la pêche) and approved by the Committee of Ethics of Bordeaux (No. 3306001).

Organotypic cultures

Organotypic hippocampal slices were prepared from 5- to 7-day-old wild-type, transgenic Thy1-YFP or transgenic Thy1-GFP mice and cultured for 2–4 weeks using the Gähwiler technique as roller-drum cultures before experiments (16). In brief, the isolated hippocampi were cut to 350 μm thickness on a tissue chopper before being embedded in plasma/thrombin clots on glass coverslips. Roller-drum culturing was done at 35°C with a rotation speed of 6/h in a medium containing 25% horse serum.

Labeling strategies

In addition to using fluorescently labeled slice cultures derived from transgenic mice, as described above, individual cells or populations of cells were labeled through complementary strategies. For co-expression of GFP and YFP in the same slices, Thy1-GFP slice cultures were transiently transfected with Lifeact-YFP carried in a Semliki-Forest viral construct, as described previously (7). For acute labeling of individual neurons, Alexa Fluor 488 and calcein-green chloride (both at final concentrations of 0.5 mM (Invitrogen, Carlsbad, CA)) were dissolved in intracellular solution containing (in mM) 125 K-gluconate, 5 KCl, 10 HEPES, 1 EGTA, 4 Mg-ATP, 0.3 Na-GTP, and 10 Na-phosphocreatine. Cells were loaded for 3–10 min in the whole-cell configuration via a patch-clamp pipette with a 4- to 5-MΩ tip resistance. In some instances, the cell remained patch-clamped for the duration of the experiment, typically ~30 min. During dye loading, the cell membrane potential was monitored in current clamp mode (I = 0 pA) to check the viability of the imaged cells. After loading, the pipette was carefully retracted, allowing the cell membrane to reseal, and, typically after an additional 5–10 min, the dye was uniformly distributed in the soma and processes. For acute cell population labeling, calcein-green acetoxymethyl (AM) ester (Invitrogen) was dissolved in artificial cerebrospinal fluid at 1 mM and injected by bolus in the CA3 area of cultures by means of a patch pipette (4- to 5-MΩ tip resistance) connected to a Picospritzer. Injections were delivered over 5–15 min as 10-ms pulses, 1–2 PSI, at 0.1 Hz. An additional 20 to 30 min were allowed to pass to ensure cleavage of the AM group in somas and diffusion of the dye into processes.

Image acquisition and analysis

The excitation and the STED beam were aligned in *x*,*y*,*z* by scanning the beams over 140-nm gold spheres and bringing the STED beam into

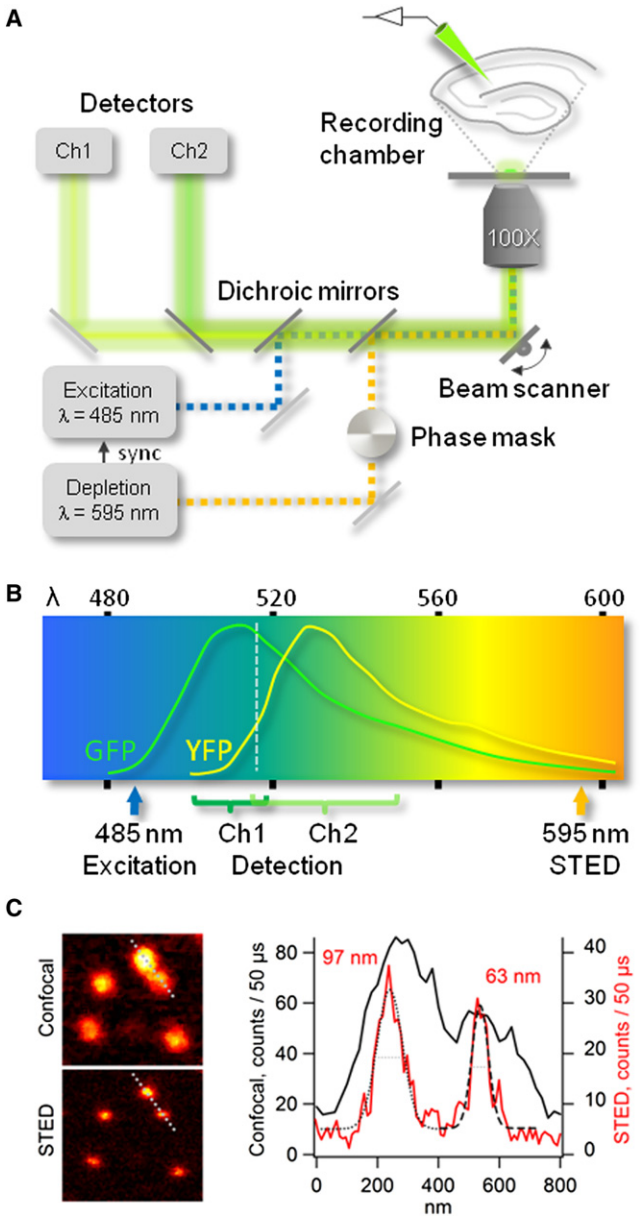

FIGURE 1 (*A*) Scheme of custom-built STED microscope. The lasers for excitation (485 nm) and depletion (595 nm) are synchronized (*small arrow*) and their beams are brought into coincidence and scanned across the brain-slice cultures in the recording chamber. A vortex phase plate imposes the doughnut shape on the depletion beam. Emitted fluorescence from the sample is descanned and split into the two detection channels on either side of the 514-nm long-pass dichroic mirror placed in front of channel 2. Removing this long-pass filter reverts the STED setup to single-channel detection. (*B*) Excitation and excited-state depletion is separated spectrally by >100 nm, leaving open a wide spectral range for fluorescence detection. The emission spectra for GFP and YFP are shown, illustrating their differing relative distribution on either side of the 514-nm long-pass filter (*dotted line*) that allows linear spectral unmixing of the two detection channels. The emission spectra for Alexa Fluor 488 and Calcein green are very similar to that of GFP (not shown). (*C*) Imaging the same frame of fluorescent beads by confocal and STED microscopy reveals the gain in spatial resolution by STED. Plots of the bead intensity profiles corresponding to the dotted lines in the images at left are depicted in the graph at right. The gain in resolution achieved by STED (*red line*, *right axis*), compared to confocal images (*black line*, *left axis*), is evident. FWHMs (*gray dotted lines*) of the three beads are calculated from Gaussian fits of the intensity profile (*black dotted and dashed lines*) and presented in the graph.

coincidence with the excitation beam using a piezo-controlled motorized mirror for the *x*,*y* plane and an adjustable telescope for alignment in *z*. Excited-state depletion was calculated as the signal ratio between *z*-scans into a sea of fluorescence (either glass cuvette or cell body) in confocal and STED modes, respectively. Microscope performance was assessed by imaging yellow-green fluorescent microspheres 40 nm in diameter coated with Alexa Fluor 488 (Invitrogen) immobilized on a glass coverslip. The same 10 μm × 10 μm frame was scanned in confocal mode and STED mode, and the full width at half maximum (FWHM) of all bead intensity profiles was calculated using the SparkMaster plugin for ImageJ (18). In the living slices, spines were typically imaged within 10 μm of the glass coverslip, and only in-focus spine necks were included for analysis. The FWHM of spine necks was calculated from manually positioned lines through the thinnest part of the neck, including all mushroom and thin spines in focus of the respective image. The intensity profile of the neck under the line was plotted and the FWHM extracted from a Gaussian fit through the pixel values. The intensity profile was calculated from 2-pixel-thick lines to reduce contributions from outlier pixels. Typical pixel size was 20 nm and typical pixel dwell time was 50 μs. Most frames were acquired as 1- to 5-μm-deep *z*-stacks typically with Δz = 300–500 nm. All imaging and cell loading was performed in a perfused imaging/electrophysiology recording chamber maintained at 32°C.

All image analysis was done on raw data, but for the figures, images were subjected to a 1-pixel median filter to suppress noise in the images from dark counts in the photodetectors. Two-color images were imported to ImageJ as 16-bit TIFF files, and spectral unmixing of fluorophores in the two channels was performed using a spectral unmixing plugin for ImageJ (19). In brief, assigning different colors (e.g., green and red) to the two raw images of either channel and merging them allowed immediate discrimination of structures labeled by the two respective fluorophores (see Figs. 4 and 6). Then, regions representing background and each of the two fluorophores were identified and selected to calculate an unmixing matrix, which was used to unmix the channels in each image section of the *z*-stack. Cross talk in the two channels was calculated as the ratio of fluorescence in the two channels from identical regions of interest containing only one fluorophore species before and after unmixing, respectively (cross talk = F_{ch1}/F_{ch2}). All results are presented as the mean ± SD. The level of significance is set at $P < 0.05$.

RESULTS

Microscope performance

The spatial resolution of the microscope setup was assessed by measuring the effective point-spread function using 40-nm fluorescent beads (Fig. 1 *C*). Imaging beads in STED mode, the average FWHM was 97 ± 20 nm, although in confocal mode it was 240 ± 67 nm. As these averages are based on all beads in the field of view, including out-of-focus beads and occasional clusters of beads, we also calculated the FWHM of the 10% best resolved among them, which was 65 ± 9 nm for the STED case and 170 ± 10 nm for the confocal case, which probably is a better estimate of the spatial resolution of the microscope.

Quenchability of YFP, GFP, Alexa Fluor 488, and calcein green fluorescence

At first, we examined the spectral dependence of the stimulated depletion of the excited state for each fluorophore. For this, we measured how much the fluorescence from a confocal spot inside a sea of fluorescence (glass cuvette or cell body) was quenched by the STED laser as a function of its wavelength (quenching = F_{STED}/F_o). The wavelength of the STED laser beam was varied via the Ti:Sa laser and the OPO, keeping the output power of the OPO constant using a Pockels cell (Conoptics, Danbury, CT). For the four fluorophores tested, the depletion was largely independent of the wavelength of the STED laser over the range 580–600 nm (Fig. 2 *A*). This was unexpected, because YFP has an emission spectrum that is shifted by ~15 nm to longer wavelengths as compared with GFP, Alexa Fluor 488, and calcein green, which have nearly identical absorption and emission spectra.

Next, we measured the dependence of fluorescence quenching on STED laser power (at 595 nm), which was similar for all fluorophores (Fig. 2 *B*). For each fluorophore, we observed a comparable level of fluorescence quenching, which was maximal at ~75–80% with the phase mask in place. In our system, this value corresponds to ~90% depletion without the phase mask, i.e., without the intensity zero at the center of the doughnut shaped beam. Taken together, these findings show that it is possible to excite and effectively deplete the fluorophores YFP, GFP, Alexa Fluor 488, and calcein green by a single excitation/depletion beam pair of 485 nm/595 nm.

Spatial resolution and fluorophore performance in living brain slices

Next, we tested all fluorophores individually with respect to their ability to achieve superresolved images of dendritic spines in living brain slices using a single set of wavelengths for fluorescence excitation and quenching, namely 485 nm for the excitation laser and 595 nm for the STED laser. To this end, neurons in organotypic hippocampal slice cultures were labeled using three different techniques: with a viral construct carrying Lifeact-YFP, via a whole-cell patch-clamp pipette (Alexa Fluor 488 or calcein green) or by the AM-ester bolus-loading technique (calcein-green AM ester). In addition, transgenic animals expressing YFP or GFP under the Thy1 promoter, primarily in CA1 pyramidal neurons, were used.

Spine necks are typically too small to be properly resolved by conventional microscopy, and can thus serve as a benchmark of imaging performance and spatial resolution. Using STED microscopy, the measured average neck width was 148 ± 401 nm (N = 53) with YFP, 151 ± 34 nm (N = 127) with GFP, 152 ± 33 nm (N = 51) with Alexa Fluor 488, and 159 ± 32 nm (N = 59) with calcein green (Fig. 3, *A–E*), consistent with previous data from

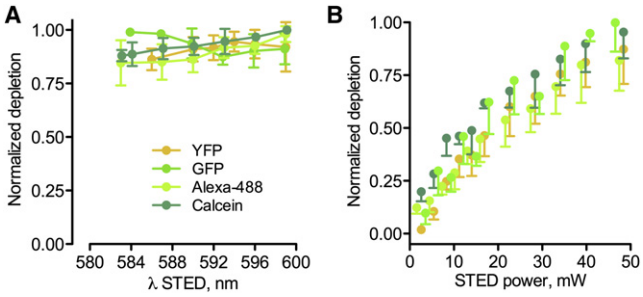

FIGURE 2 (*A*) Depletion of YFP, GFP, Alexa Fluor 488, and Calcein green is largely independent of the depletion wavelength over the range 580–600 nm. The spectra were recorded at constant depletion power (~42 mW into the aperture of the objective, with phase mask in place) and normalized to the maximum depletion achieved for each fluorophore. (*B*) Fluorescence depletion of the fluorophores measured inside living neurons in brain slices as a function of STED laser power at the back aperture of the objective. All values are normalized to the maximum depletion of GFP to facilitate comparison across fluorophores. The curves were recorded at 595 nm and under identical conditions. A maximal depletion of 89% was achieved for Alexa Fluor 488 at ~50 mW of STED laser power (without phase mask).

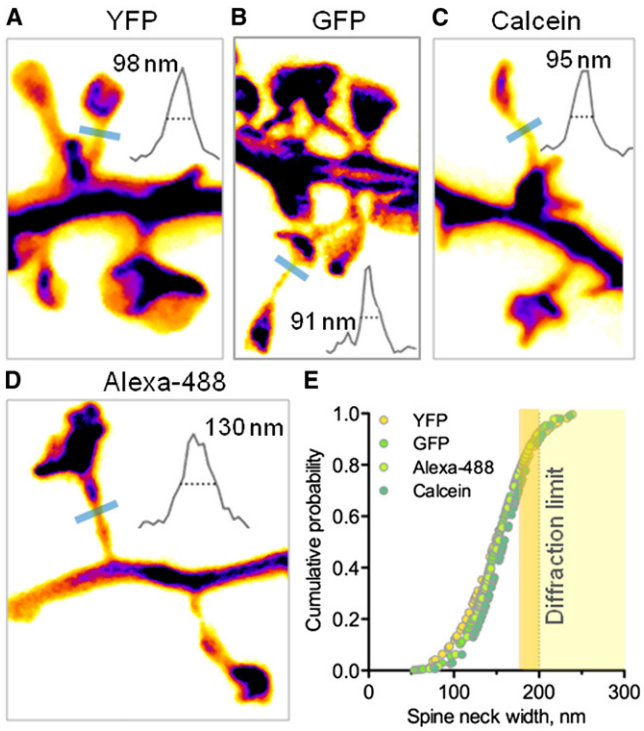

FIGURE 3 (*A–D*) Examples of spine necks imaged using YFP (*A*), GFP (*B*), calcein green (*C*), and Alexa Fluor 488 (*D*) as volume labels of spine morphology. The profile plots of the blue bars across the spine necks (*insets*) illustrate that superresolved images can be acquired with all four fluorophores using the same excitation (485 nm) and depletion (595 nm) wavelengths. (*E*) Cumulative probability plot of spine neck widths of all mushrooms and thin spines in focus in the analyzed images, obtained with the four respective fluorophores. It is clear that the majority of spine necks are thinner than what can be resolved with conventional diffraction-limited techniques (diffraction limit indicated by yellow bar). Student unpaired *t*-tests returned no significant differences between the neck widths reported by the four fluorophores, suggesting that they are equally well suited for imaging dendritic spine neck morphology under the given settings.

superresolution imaging (6) and electron microscopoy analyses (20). As a conservative estimate of the resolution gain for each fluorophore, we calculated the top 10% of thinnest spine necks, which were 86 ± 9 nm (N = 5) with YFP, 77 ± 19 nm (N = 13) with GFP, 89 ± 19 nm (N = 5) with Alexa Fluor 488, and 100 ± 15 nm (N = 6) with calcein green. Student *t*-test results indicated no significant width differences between the average and the top 10% of resolved necks of each fluorophore. Taken together, the data demonstrate that superresolved images can be acquired using any of the dyes at the same set of excitation and STED laser wavelengths, and that it is not necessary to use different wavelengths to achieve effective quenching and hence produce a gain in spatial resolution.

Two-color STED imaging of living synapses using a single laser-beam pair

We then simultaneously imaged pre- and postsynaptic structures expressing purely YFP or GFP, yielding superresolved images, as predicted (Fig. 4 *A*). Simply by adding a dichroic mirror in front of a second detector, it becomes possible to distinguish well which structures express YFP or GFP (Fig. 4 *B*). As expected for spectral detection of GFP and YFP using a 514-nm long-pass emission filter, the GFP signal was equally strong in both detection channels, whereas the YFP signal was more dominant in the longer-wavelength channel. The ratio of GFP signal in channel 1 to that in channel 2 was 0.92 ± 0.04 before unmixing, and 0.10 ± 0.06 (N = 3) after unmixing. For YFP, the corresponding ratios were 0.27 ± 0.01 and 0.09 ± 0.02 (N = 9) (see Fig. 7). Taken together, performing linear spectral unmixing makes the spectral separation between the YFP and GFP signals very effective, reducing the fluorescent cross talk in the detection channels to ~10% (Fig. 4 *C*; and see Fig. 7).

Repeated imaging of YFP- and GFP-labeled synaptic structures demonstrates that pre- and postsynaptic structures can be effectively spectrally separated and imaged simultaneously with subdiffraction spatial resolution (>100 nm) over a period of several tens of minutes without any changes in image quality and sample viability (Fig. 5, *A–F*).

Next, we examined whether it is possible to replace GFP with the other dyes and labeling approaches and achieve the same results for dual labeling with YFP. Indeed, imaging YFP alongside Alexa Fluor 488 (Fig. 6, *A–C*) or calcein green (Fig. 6, *D–F*) also yielded superresolved images in both channels, easy discrimination of fluorophores based on raw data alone and effective spectral separation after unmixing of the detection channels. Calcein was used successfully in these experiments, either when loaded into cells via a patch pipette (Fig. 3 *C*, *spines*) or when bolus-loaded in its ester form (Fig. 6, *D–F*, *axons*). The cross-talk ratios of Alexa Fluor 488 in the two channels before and after unmixing, respectively, are 0.58 ± 0.02 and 0.10 ± 0.03 (N = 3), and those for calcein green are 0.60 ± 0.02 and 0.10 ± 0.04 (N = 4). Taken together, these results demonstrate that two-color STED images can be readily obtained for these popular green dyes and that the fluorescence signals can be spectrally unmixed to at least 90% purity (Fig. 7).

DISCUSSION

Our study presents a straightforward and powerful way to perform STED imaging in two colors, which is compatible with standard fluorophores and which does not require a complex or costly redesign of the STED setup. As we performed all experiments with pulsed-laser sources, it remains

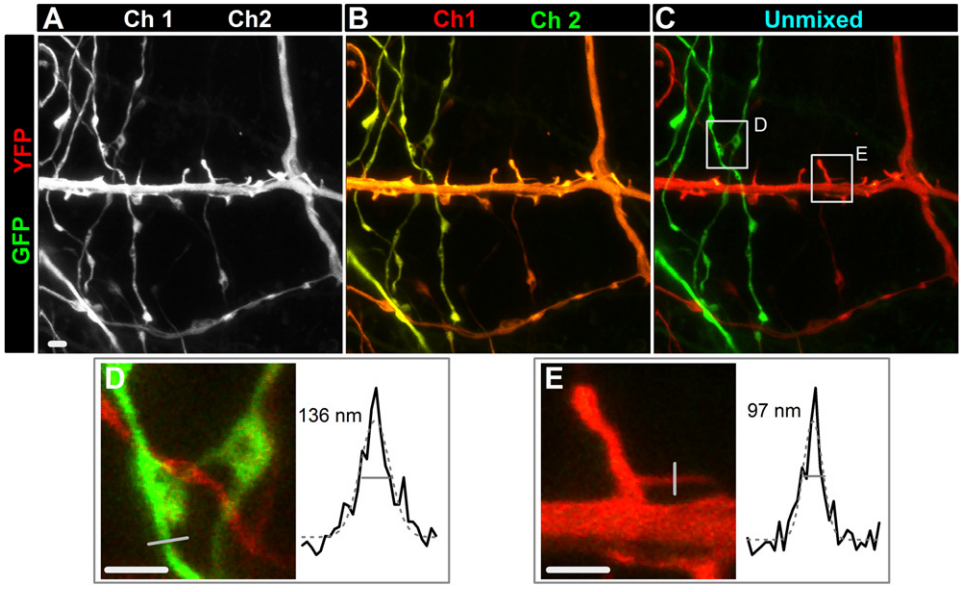

FIGURE 4 (*A*) YFP and GFP imaged together in two channels but merged using a gray lookup table. (*B*) The two-channel raw data merged in red and green colors, respectively. It is noteworthy that from merging the two mixed channels in different colors, structures expressing either YFP or GFP can already be readily discriminated due to their differing relative contribution in each of these. (*C*) Linear unmixing of the two fluorophores results in clear separation of these structures, leaving <10% residual cross talk in the channels. (*D* and *E*) Zoom-ins of the outlined regions in *C*, depicting examples of superresolved structures labeled by GFP (*D*) and YFP (*E*), along with their corresponding line intensity plots and FWHM values. Scale bars, 1 μm.

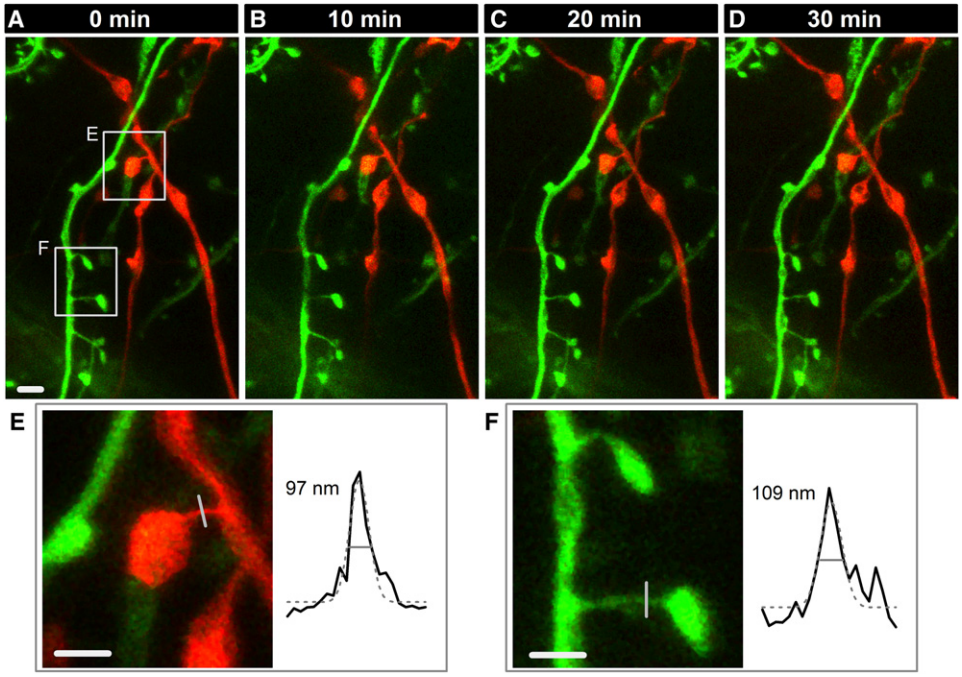

FIGURE 5 Time-lapse *z*-stack imaging of YFP (*red*) and GFP (*green*) synaptic structures did not result in any apparent photodynamic damage. Fluorophore bleaching was not an issue, presumably because the fluorophores are freely diffusible, allowing for replenishment even after bleaching. All frames depict maximal intensity projections of *z*-stacks. (*E* and *F*) Magnifications of the outlined structures in *A*, illustrating that both fluorophores are superresolved in the images. Scale bars, 1 μm.

to be seen whether continuous-wave lasers, which are cheaper and easier to handle, can also be used for the two-color STED imaging approach we have described here (21).

STED microscopy was introduced more than a decade ago; however, its use in cell biology and neuroscience research is still fairly limited, despite its ground-breaking potential as a live-cell superresolution imaging technique. Its adoption has been hampered by the view of many biologists that its design is too complex, or its scope too limited, to be worth implementing in their own labs. This view is bound to change as technical improvements make STED microscopy less complicated and versatile.

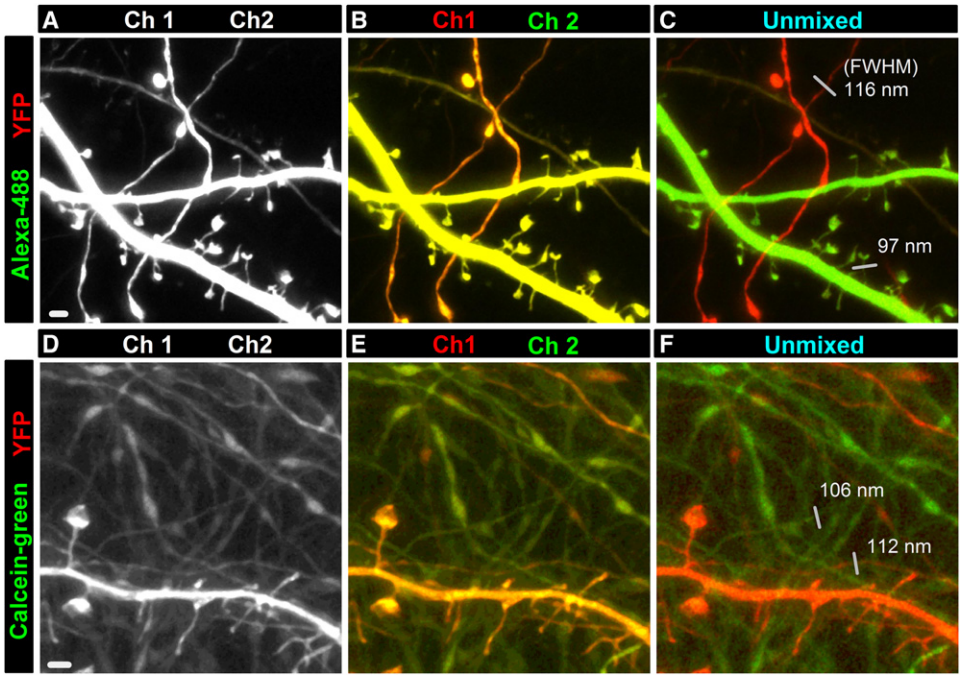

FIGURE 6 (*A*) Two detection channels merged when imaging YFP and Alexa Fluor 488. (*B*) As described, by assigning red to one channel and green to the other, structures labeled by either of the two fluorophores can be readily discriminated. (*C*) The linearly unmixed fluorophores are unambiguously separated, revealing axonal structures genetically labeled by YFP and two crossing dendrites whole-cell labeled with Alexa Fluor 488. The FWHMs of the intensity profiles of the two white lines illustrate that both fluorophores are superresolved in the image. (*D–F*) Images of slices colabeled with YFP and calcein green. The two fluorophores are easily distinguishable simply by assigning different colors to the two detection channels (*E*), and linear unmixing can clearly separate the fluorophore signals (*F*). Among the dense network of calcein-green-labeled axons in *F*, a few YFP (*red*) axons can be seen, which may originate from the same cell as the genetically YFP-labeled dendritic segment displayed or from other YFP-expressing cells in the slice culture. Again, as seen from the FWHMs of the depicted line profiles in *F*, both fluorophores are superresolved. The relatively high signal background in the calcein-green channel (*D–F*) stems from the ester-loading procedure, where many cells are loaded around the bolus injection site. Images are maximum-intensity projections of *z*-stacks. Scale bars, 1 μm.

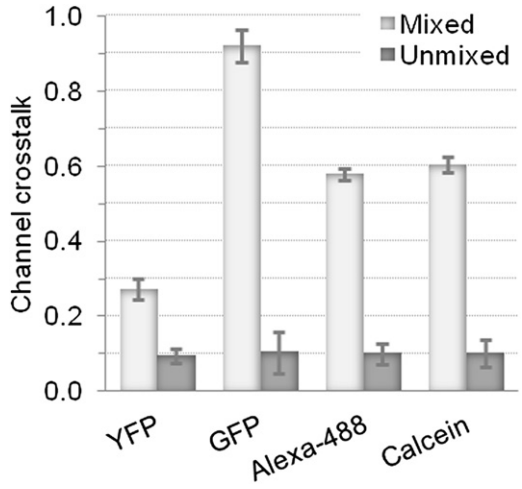

FIGURE 7 Channel cross talk before and after unmixing of the fluorophores, expressed as the ratio of signal intensity for the same region in the two detection channels. Before unmixing, the channel ratios of the four respective fluorophores differ, in agreement with their emission spectra and the 514-nm long-pass emission filter. Unmixing effectively separates the fluorophores into separate channels, leaving ~10% residual cross talk regardless of the initial signal ratios.

Thus, we have striven to develop a way to achieve two-color separation for STED imaging that makes it straightforward in a way similar to conventional and other superresolution microscopy techniques, such as PALM/STORM or SIM (22).

Although both GFP and YFP have been successfully used for STED microscopy (6,23), to our knowledge, no attempt has been made to image them at the same time. Previously, the laser wavelength used to quench GFP was ~570 nm (23,24), whereas for YFP it was ~600 nm (6). Here, to our knowledge, we show for the first time that GFP and YFP, as well as Alexa Fluor 488 and calcein green, are equally quenchable between 580 and 600 nm, the range being defined by the tunability of our laser rather than fluorophore performance. This makes it possible to select a single wavelength for the STED laser (595 nm in our case) to quench all of these fluorophores in one go. Combined with spectral detection and unmixing, intrinsically aligned two-color nanoscale imaging can be achieved, forgoing the need for more complex strategies, which may not be compatible with the dyes used in this study.

Compared to two-color approaches relying on three or more beams, it is much easier to operate and maintain a setup with a single beam pair. In addition, the single-beam-pair/unmixing approach also offers more flexibility for integrating complementary optical techniques such as two-photon uncaging or optogenetics, as a broader spectral range is left available for these.

The strength of using only a single beam pair for STED imaging also relates to the inherent temporal and spatial coincidence of fluorescence excitation and quenching for both fluorophores, which distinguishes our method from previous two-color solutions (8–11). Moreover, considering the limited selection of fluorophores currently available for two-color STED imaging, in particular for live-cell imaging, the ability to use YFP together with GFP, Alexa Fluor 488, or calcein green should be a welcome complement to existing two-color superresolution strategies.

As we did not need to increase the laser power for the two-channel recordings, there was no increase in the likelihood of inducing photodynamic damage, offering an advantage over using extra beams to excite more than one fluorophore (8–10) or having to excite and quench two fluorophores successively in time (11). Acquiring z-stacks of images, we could readily carry out prolonged time-lapse imaging with YFP and GFP without any apparent signs of phototoxicity. As a cautionary note, we did occasionally observe signs of damage during more intense image acquisitions (larger fields of views or more time points) when using calcein green as a label, and also (but less frequently so) in the case of Alexa Fluor 488.

Another advantage is the ease of switching between single-channel and two-channel recordings, which can be done repeatedly over the course of an experiment, as the 514-nm dichroic mirror can be accurately moved in and out of the detection light path. It will be interesting to apply this strategy for achieving multicolor superresolution imaging to other dyes, which are also excitable and quenchable by one set of wavelengths. Adding more detection channels may make it possible to separate the fluorescence signals of more than two dyes simultaneously if the signals are strong enough to be divided among three or more detectors.

Although the raw two-channel data already give a clear indication as to which dye is present in the structures, unmixing the images allows experimenters to further disambiguate structures that are in close contact or that overlap in the z axis. The results achieved by linear unmixing were comparable for all fluorophores we examined, with residual color cross talk 10% or less after unmixing. Iterative unmixing or using more refined algorithms may improve the unmixing results even further. Therefore, we are optimistic that yellow/green fluorophore unmixing can also be performed on interspersed fluorophores, e.g., for colocalizing synaptic proteins within a volume-labeled synaptic structure.

Using an oil microscope objective, we imaged spines with necks thinner than 70 nm within 10 μm from the surface of the coverslips on which the brain-slice cultures were mounted. Focusing deeper into the slice, the images quickly degraded in spatial resolution, which is expected given the mismatch in refractive indices between the oil-immersion medium and the brain tissue. We have recently demonstrated that the use of a glycerol-immersion objective with a correction collar can effectively reduce the aberrations associated with this mismatch, permitting nanoscale imaging up to 100 μm deep inside living brain slices (7). Our two-color approach should be readily compatible with the use of a glycerol objective.

In summary, we demonstrate that it is possible to achieve two-color STED superresolution imaging in living brain slices using combinations of the popular green fluorophores YFP, GFP, Alexa Fluor 488, and calcein green using a single beam pair for excitation and quenching at 485 nm and 595 nm, respectively, and adding a second detector using standard optical components. The signals from the two detection channels can be readily unmixed with freely available software, allowing for effective separation of the fluorophores, using several labeling strategies based on transgenics and physical loading using patch pipettes. We illustrated the potential of our approach by two-color imaging of dendritic and axonal segments in living-brain slices, facilitating investigations into the morphological plasticity of neurons and glia at the nanoscale inside living and intact brain tissue preparations.

We thank E. Avignone, A. Panatier, and S. W. Hell for comments on the manuscript, and J. Angibaud and R. Chereau for technical support. We thank G. Beck for the Lifeact-YFP construct.

This work was supported by a postdoctoral project grant from the Lundbeck Foundation to J.T., and grants from the Institut National de la Santé et de la Recherche Médicale, the Agency of Natural Resources, and the Human Frontier Science Program to U.V.N.

REFERENCES

1. Hell, S. W., and J. Wichmann. 1994. Breaking the diffraction resolution limit by stimulated emission: stimulated-emission-depletion fluorescence microscopy. *Opt. Lett.* 19:780–782.
2. Klar, T. A., S. Jakobs, …, S. W. Hell. 2000. Fluorescence microscopy with diffraction resolution barrier broken by stimulated emission. *Proc. Natl. Acad. Sci. USA.* 97:8206–8210.
3. Kittel, R. J., C. Wichmann, …, S. J. Sigrist. 2006. Bruchpilot promotes active zone assembly, Ca^{2+} channel clustering, and vesicle release. *Science.* 312:1051–1054.
4. Sieber, J. J., K. I. Willig, …, T. Lang. 2006. The SNARE motif is essential for the formation of syntaxin clusters in the plasma membrane. *Biophys. J.* 90:2843–2851.
5. Westphal, V., S. O. Rizzoli, …, S. W. Hell. 2008. Video-rate far-field optical nanoscopy dissects synaptic vesicle movement. *Science.* 320: 246–249.
6. Nägerl, U. V., K. I. Willig, …, T. Bonhoeffer. 2008. Live-cell imaging of dendritic spines by STED microscopy. *Proc. Natl. Acad. Sci. USA.* 105:18982–18987.
7. Urban, N. T., K. I. Willig, …, U. V. Nägerl. 2011. STED nanoscopy of actin dynamics in synapses deep inside living brain slices. *Biophys. J.* 101:1277–1284.
8. Donnert, G., J. Keller, …, S. W. Hell. 2007. Two-color far-field fluorescence nanoscopy. *Biophys. J.* 92:L67–L69.
9. Meyer, L., D. Wildanger, …, S. W. Hell. 2008. Dual-color STED microscopy at 30-nm focal-plane resolution. *Small.* 4:1095–1100.
10. Bückers, J., D. Wildanger, …, S. W. Hell. 2011. Simultaneous multi-lifetime multi-color STED imaging for colocalization analyses. *Opt. Express.* 19:3130–3143.
11. Willig, K. I., A. C. Stiel, …, S. W. Hell. 2011. Dual-label STED nanoscopy of living cells using photochromism. *Nano Lett.* 11:3970–3973.
12. Neher, R., and E. Neher. 2004. Optimizing imaging parameters for the separation of multiple labels in a fluorescence image. *J. Microsc.* 213:46–62.
13. Zimmermann, T., J. Rietdorf, and R. Pepperkok. 2003. Spectral imaging and its applications in live cell microscopy. *FEBS Lett.* 546:87–92.
14. Nägerl, U. V., and T. Bonhoeffer. 2010. Imaging living synapses at the nanoscale by STED microscopy. *J. Neurosci.* 30:9341–9346.
15. IMSpector. www.max-planck-innovation.de/de/industrie/technologieangebote/software/.
16. Gähwiler, B. H. 1981. Organotypic monolayer cultures of nervous tissue. *J. Neurosci. Methods.* 4:329–342.
17. Reference deleted in proof.
18. Picht, E., A. V. Zima, …, D. M. Bers. 2007. SparkMaster: automated calcium spark analysis with ImageJ. *Am. J. Physiol. Cell Physiol.* 293:C1073–C1081.
19. Unmixing. http://rsbweb.nih.gov/ij/plugins/spectral-unmixing.html.
20. Harris, K. M., and S. B. Kater. 1994. Dendritic spines: cellular specializations imparting both stability and flexibility to synaptic function. *Annu. Rev. Neurosci.* 17:341–371.
21. Willig, K. I., B. Harke, …, S. W. Hell. 2007. STED microscopy with continuous wave beams. *Nat. Methods.* 4:915–918.
22. Toomre, D., and J. Bewersdorf. 2010. A new wave of cellular imaging. *Annu. Rev. Cell Dev. Biol.* 26:285–314.
23. Willig, K. I., R. R. Kellner, …, S. W. Hell. 2006. Nanoscale resolution in GFP-based microscopy. *Nat. Methods.* 3:721–723.
24. Rankin, B. R., G. Moneron, …, S. W. Hell. 2011. Nanoscopy in a living multicellular organism expressing GFP. *Biophys. J.* 100:L63–L65.